Rheological Performance And Microstructural Characteristics Of Modified Asphalt Binder

Ahmad Septiawan[1], Sigit Pranowo Hadiwardoyo[1*], R. Jachrizal Sumabrata[1], and Riana Herlina Lumingkewas[2]

[1] Department of Civil Engineering, Universitas Indonesia, Kampus UI Depok 16424, Indonesia
[2] Civil Engineering Study Program, Institut Teknologi Indonesia, Tangerang Selatan, Indonesia
[*] Corresponding author. E-mail: sigit@eng.ui.ac.id

Received: Apr. 04, 2026; Accepted: Jul. 19, 2026

Although numerous studies have evaluated asphalt modifiers, systematic comparisons of multiple micro-scale additives under an identical experimental framework remain limited. To address this gap, this study analyzed the rheological performance and microstructural characteristics of asphalt binders modified with four micro-material additives: fly ash (FA), cement (Ce), crumb rubber (Cr), and silica (Si). Particle size reduction was carried out by milling, producing micro-scale particles, which were then blended with pure asphalt pen 60/70 (PG-64) at dosages of 1–3%. Performance was evaluated using conventional physical tests, rotational viscosity, Scanning Electron Microscope (SEM), and Dynamic Shear Rheometer (DSR) tests, including temperature sweeps under three aging conditions: original, RTFO and PAV. Results showed that the micro-material modifiers significantly affected the physical and rheological characteristics of asphalt binders, reducing penetration values, raising softening points and enhancing viscoelastic performance across aging conditions. Temperature strongly influences binder viscosity, with higher temperatures producing lower viscosity and varying levels of temperature sensitivity among binders. The modified binders, including Cement (VCe), Fly Ash (VFA), Crumb Rubber (VCr) and Silica (VSi) exhibited increased complex modulus (G^*) and reduced phase angle (δ), indicating improved stiffness, structural stability, and elastic behavior. Rheological evaluation further revealed that increasing temperature reduced rutting and fatigue performance, while modified binders generally exhibited lower fatigue parameter ($G^* \sin\delta$) values than the virgin binder, indicating enhanced fatigue cracking resistance. The VCr mixture, particularly VCr-3, demonstrated the most effective improvement in long-term fatigue resistance and elastic performance.

Keywords: micro-material, modified asphalt binder, rheology, temperature sweep

http://dx.doi.org/10.6180/jase.202611_34.005

1. Introduction

Permanent deformation is one of the most critical forms of damage in flexible pavements. It occurs due to the accumulation of plastic strain in the asphalt layer under repeated traffic loads and high operating temperatures [1, 2]. This condition causes decreased driving comfort, reduced road user safety, and increased pavement maintenance costs throughout its service life [3, 4]. The rutting phenomenon is a primary indicator of structural fatigue in the surface layer, where the viscoelastic behavior of the binder plays an equally important role as the gradation and mixture structure characteristics [5, 6]. Microstructurally, the behavior of the asphalt binder, which functions as a binding matrix between aggregates, greatly influences permanent deformation [7]. A binder with a good viscoelastic balance can withstand strain at high temperatures and recover its shape after the load is released, whereas a binder with excessive stiffness or low elasticity tends to exhibit irreversible plastic flow [8, 9]. Several previous studies have shown that the resistance of pavements to permanent deformation depends not only on the aggregate gradation and mixture density but is also greatly influenced by the binder's basic properties [10, 11].

Binder rheological characteristics and aggregate size distribution play a major role in determining rutting resistance in asphalt layers [12]. Variations in binder type and stiffness contribute significantly to the mixture's ability to withstand plastic deformation [13]. A balanced viscoelasticity enables it to withstand deformation at high temperatures while maintaining elastic properties, enabling recovery after the load is removed [14]. For decades, asphalt quality assessments across various specifications have relied on conventional parameters such as penetration tests, softening point, and ductility [15, 16]. Therefore, analyzing the relationship between binder rheology and permanent deformation resistance is crucial for developing modern pavement materials that are adaptive to extreme thermal conditions and traffic loads [17].

Adding nanomaterials to modified asphalt can enhance its performance at high temperatures and rutting resistance [18]. Extensive research has been conducted on the development of nanomaterial technology as additives in asphalt mixtures. Haroon et al. (2024) conducted a study incorporating silica nanomaterials at five doses (1–5% by weight of bitumen) into 10% crumb-rubber (CR) modified bitumen using a wet-mixing technique. The asphalt test results showed that this modification improved performance against rutting and fatigue damage as the nanomaterial content increased [19]. A higher percentage of nanomaterials increased the recovery rate and, at different stress levels, could reduce non-recoverable creep compliance [20, 21]. Other studies have shown that adding nanomaterials to asphalt mixtures can improve performance against permanent deformation [22–24]. The incorporation of modified crumb rubber and surfactants was reported to improve the mechanical properties of asphalt binders [25]. In addition, modifying rubberized asphalt with 3-triethoxysilyl propylamine (3-tri) showed that the addition of 0.5% additive enhanced its rutting resistance [26]. Increasing the crumb rubber content increased viscosity while reducing penetration and ductility. Based on the rutting resistance and non-recoverable creep compliance (Jnr) results, a crumb rubber content of 10% was identified as the optimum proportion [27]. Crumb rubber-modified binders with higher rubber proportions exhibited increased viscosity and a lower risk of cracking damage under low-temperature conditions [28]. Increasing the crumb rubber content in virgin asphalt binders was found to raise the binder failure temperature [29]. Asphalt mixtures modified with 1% and 2% nano-silica (NS) and 1% nano-fly ash (NFA) were evaluated and the results showed that the addition of 1% NS increased the complex modulus (G^*) of the asphalt binder and improved its rutting resistance compared with the control asphalt [30]. Most prior studies, however examined a single modifier in isolation and under a limited range of aging conditions, leaving little comparative evidence on how chemically distinct materials perform under an identical protocol. Moreover, the literature rarely combines a pozzolanic material, a hydraulic binder, an elastomeric material and a mineral filler within one controlled framework, despite each representing a distinct modification mechanism. This gap limits evidence-based modifier selection for specific climatic or traffic conditions and leaves open whether micro-scale, rather than nanoscale, particle reduction can still yield meaningful performance gains at lower processing cost. This study addresses this gap by systematically comparing four micro-scale materials FA, Ce, Cr and Si produced via uniform ball-milling and evaluated under identical physical, rheological (DSR) and microstructural (SEM) testing across three aging states (Unaged, RTFO, PAV). The objectives of this study were, first, to analyze the effect of adding micro-particles on changes in the physical properties of the binder. Second, to identify the morphology of microparticles and their contribution to changes in the microstructure of the binder and thirdly, to analyze the rheological behavior under three aging conditions (original, RTFO, PAV) through the parameters G^*, δ, rutting parameter ($G^* / \sin\delta$) and fatigue parameter ($G^* \sin\delta$).

2. Materials and methods

2.1. Materials

The pure asphalt used in this study was of penetration grade 60/70 or PG-64 (Table 1). The powder materials used in this study included silica (Si), crumb rubber (CR), cement (Ce) and fly ash (FA) (Fig. 1). These powder materials were obtained from commercial suppliers that generally offer similar products.

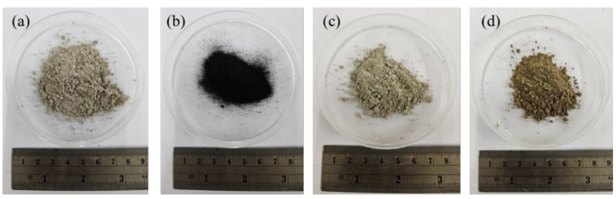

Fig. 1. Powder material (a) Si; (b) Cr; (c) Ce and (d) FA

Table 1. Basic properties of virgin binder

No.	Type of Testing	Testing Method	Result	Unit
1	Penetration at 25 °C	ASTM D-5	68.7	0.1 mm
2	Softening Point	ASTM-D36	48.5	°C
3	Flash Point	ASTM D-92	328	°C
4	Ductility at 25 °C	ASTM-D113	165+	cm
5	Viscosity at 135 °C	AASHTO T-316	0.522	Pa·S
6	Density at 25 °C	AASHTO T-228	1.03	gr/cc

2.2. Preparation of micromaterials

The powder was first sieved to $\leq$ 0.075 mm as the starting material for the size-reduction process. This dry sieving step was performed without the addition of any surfactant or anti-agglomeration agent. After the screening process was completed, the next step was grinding using a simple ball mill equipped with two types of steel balls: 15 mm (42.04 grams) and 8 mm (20.88 grams), each with a total of six pieces (Fig. 2). Grinding was carried out continuously under dry-milling conditions for $\pm$20 hours at a rotational speed of 80 rpm, without any anti-agglomeration agents or process control additives yielding the particle sizes shown in Table 2. The resulting average particle sizes confirm that this dry, low-speed protocol was suffient to achieve the target micro-scale particle range.

Table 2. Particle size

Materials	Particle size (μm)		
	Min.	Max.	Average
Silica	0.275	7.340	1.389
Crumb-rubber	0.223	7.640	1.180
Cement	0.296	5.703	1.236
Fly-ash	0.247	4.662	0.953

2.3. Sample of modified binders

Mixing speeds and durations for incorporating micro-scale additives into asphalt binders have been widely reported in the literature. Crumb rubber-modified binders prepared using a high-shear mixer at 2,000 rpm for 60 min exhibited homogeneous particle dispersion and consistent rheological improvements [31]. Similarly, mixing micro-silica powder with asphalt binder at 2,000 rpm, combined with an adequate mixing duration, was reported to produce uniform dispersion of micro-scale silica particles while reducing agglomeration [32]. Moreover, shear mixing at 2,000 rpm for 75–120 min was found to be applicable to various inorganic and elastomeric modifiers, including crumb rubber and fly ash-based geopolymer, indicating the suitability of this mixing speed for additives with different modification mechanisms [33]. Modified binders were prepared by adding micromaterials to pure 60/70 asphalt. The pure asphalt was heated for approximately 30 minutes to 150 °C $\pm$ 5 °C, then the micro powder is slowly added at that temperature. Mixing was carried out at 2,000 rpm for 60 minutes to ensure homogeneity of the mixture.

Table 3. Sample marks of asphalt modification

Binder composition	Sample marks		
	1%	2%	3%
Virgin binder + FA	VFA-1	VFA-2	VFA-3
Virgin binder + Ce	VCe-1	VCe-2	VCe-3
Virgin binder + Cr	VCr-1	VCr-2	VCr-3
Virgin binder + Si	VSi-1	VSi-2	VSi-3

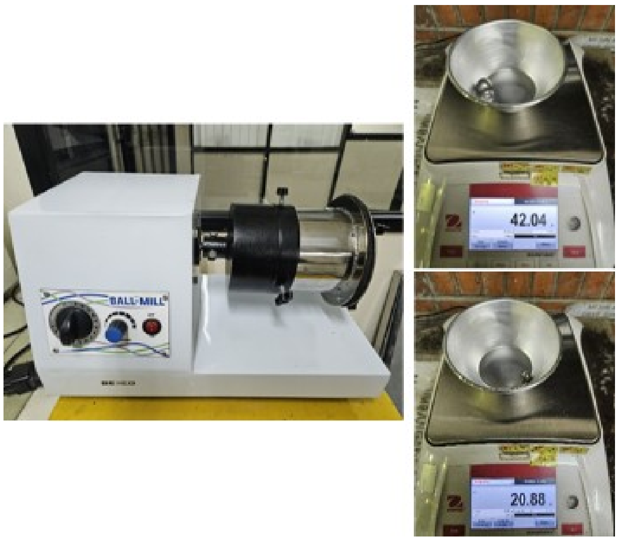

Fig. 2. Ball-mill

2.4. Scanning electron microscope (SEM) test

Additive measurements were carried out using a Hitachi SU3500 machine with a magnification of 15,000×. Surface analysis using SEM will provide visual data obtained from a surface layer of approximately 20 μm from the observed surface [34].

2.5. Rotational viscosity test

The values obtained from viscosity are in accordance with the AASHTO T316 standard [35]. According to AASHTO M320, the standard specifications for performance-rated asphalt binders, the viscosity should not exceed 3 Pa·s at 135 °C [36]. The evaluation of temperature susceptibility to viscosity is shown in the following Eq. (1).

$$\mathrm{Log}(\log(\eta \times 10^3)) = n - m\log(T + 273.13) \qquad (1)$$

η is the dynamic viscosity (mPa·S). T is the temperature (°Celsius). m and n are the regression coefficients.

2.6. Dynamic shear rheometer (DSR) test

Rheology tests were conducted on samples with a diameter of 8 mm and a thickness of 2 mm [37]. In this study, temperature sweep tests were conducted with a fixed frequency of 10 rad/s or 1.59 Hz and a test temperature range from 24 °C to 80 °C with an 8 °C interval difference and were conducted at three age conditions, namely original (unaged), short-term aging (RTFO) and long-term aging (PAV). The purpose of this analysis was to evaluate the impact of aging on the viscoelastic characteristics of asphalt binders and to determine the response of undamaged materials in various temperature ranges [38]. The relationship between rutting parameter ($G^* / \sin\delta$) and fatigue parameter ($G^* \sin\delta$) with temperature and percentage is calculated using the following power law formula (Eq. (2)):

$$G^* / \sin\delta \text{ or } G^* \sin\delta = a \cdot T^b \cdot P^c \qquad (2)$$

T represents temperature and P represents the additive content, while a, b and c are regression coefficients obtained from the model fitting process. The coefficient (a) represents the initial magnitude or baseline level of the rheological parameter being modeled. Higher values of (a) generally indicate greater stiffness or higher resistance of the asphalt binder under the test conditions. The coefficient (b) describes the sensitivity of the rheological parameter to temperature variations, where a smaller value of (b) indicates lower temperature susceptibility of the modified asphalt binder. Meanwhile, the coefficient (c) represents the influence of additive content on the rheological response. A positive value of (c) indicates that increasing the additive dosage enhances the rheological parameter, whereas a negative value indicates that increasing the additive dosage reduces the rheological response.

3. Results and discussions

3.1. Morphology analysis

FA particles (Fig. 3 a) appear relatively smooth on the surface and have hundreds of nanometers. Si particles (Fig. 3 b) exhibit highly irregular, sharp-angled and rough-textured particles. Cr (Fig. 3 c) exhibits irregularly geometric particle clumps with porous surfaces and a fibrous appearance. Ce (Fig. 3 d) exhibits angular particles that tend to form dense clumps. These morphological differences indicate that the four materials differ not only in shape and surface texture but also in their interaction mechanisms and contribution to the microstructural and macroscopic performance of the mixture.

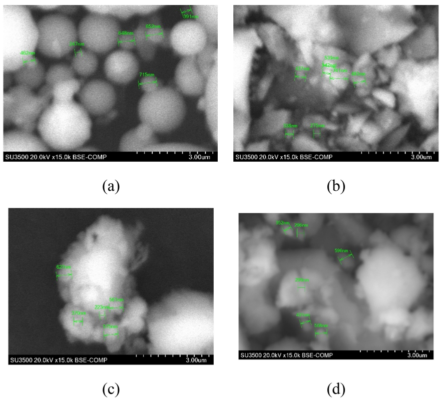

Fig. 3. SEM images (a) FA; (b) Si; (c) CR and (d) Ce

3.2. Analysis of physical characteristics

The pattern of penetration reduction or stiffening effect significantly increases with increasing percentage of additive material in the binder, with a decrease ranging 5–15% (Fig. 4 a). The VFA mixture shows a penetration reduction of around 5–7%; the VCe and VSi mixtures, around 10–13%; and the VCr mixture, around 14–15%, although the penetration value is the highest.

The increasing trend in softening point values (Fig. 4 b) indicates increased material resistance to deformation and reduced sensitivity to high temperatures. Increasing the blend percentage from 1–3% increases softening point values across all material variations, with the magnitude of the increase ranging from 4–10%. The VFA blend showed the highest increase, at around 8–10%. The VCe and VSi blends experienced relatively moderate increases of 5–7%. Meanwhile, VCr showed a modest increase of 4–5%.

Table 4. Viscosity-temperature sensitivity for modified binder

Binder types	The relationship between sensitivity of viscosity and temperature	R^2
Virgin	Log (log($\eta \times 10^3$)) = 9.72 – 3.56 log (T+273.13)	0.99
VFA-1	Log (log($\eta \times 10^3$)) = 8.57 – 3.11 log (T+273.13)	0.99
VFA-2	Log (log ($\eta \times 10^3$)) = 9.38 – 3.42 log (T+273.13)	0.99
VFA-3	Log (log ($\eta \times 10^3$)) = 9.39 – 3.43 log (T+273.13)	0.99
VCe-1	Log (log ($\eta \times 10^3$)) = 10.07 – 3.69 log (T+273.13)	0.99
VCe-2	Log (log ($\eta \times 10^3$)) = 9.37 – 3.41 log (T+273.13)	0.99
VCe-3	Log (log ($\eta \times 10^3$)) = 9.49 – 3.46 log (T+273.13)	0.98
VCr-1	Log (log ($\eta \times 10^3$)) = 9.02 – 3.28 log (T+273.13)	0.99
VCr-2	Log (log ($\eta \times 10^3$)) = 9.62 – 3.52 log (T+273.13)	0.99
VCr-3	Log (log ($\eta \times 10^3$)) = 8.45 – 3.05 log (T+273.13)	0.99
VSi-1	Log (log ($\eta \times 10^3$)) = 8.98 – 3.27 log (T+273.13)	0.99
VSi-2	Log (log ($\eta \times 10^3$)) = 9.97 – 3.65 log (T+273.13)	0.99
VSi-3	Log (log ($\eta \times 10^3$)) = 9.52 – 3.48 log (T+273.13)	0.99

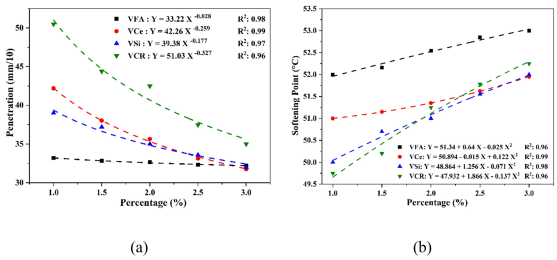

Fig. 4. The relationship between: (a) penetration and (b) softening point with the additive percentage

3.3. Relationship between viscosity and temperature

Table 4 shows the relationship between viscosity (η) and temperature (T) for various binders using a log–log regression model. In general, all binders exhibit a negative relationship between viscosity and temperature, as indicated by a negative slope coefficient in the equation. This indicates that viscosity decreases with increasing temperature.

The slope coefficient values ranged from –3.05 to –3.69, indicating differences in the temperature sensitivity of viscosity for each binder. Binders with larger slope values exhibited higher temperature sensitivity than those with smaller slopes. Among the modified binders, VCe-1 (–3.69) and VSi-2 (–3.65) exhibited steeper slopes than the virgin binder (–3.56), indicating a greater reduction in viscosity with increasing temperature. This behavior may be attributed to the predominantly mineral nature of cement and silica particles, which primarily contribute through a stiffening or filler effect at lower temperatures. As temperature increases, the contribution of these rigid particles to the overall binder viscosity becomes less pronounced, resulting in a faster decrease in viscosity and consequently higher temperature susceptibility.

In contrast, VCr-3 exhibited the lowest slope value (–3.05), suggesting improved viscosity stability over the tested temperature range. This behavior is likely associated with the elastomeric characteristics of crumb rubber, which can absorb light fractions from the asphalt binder and develop a swelling effect, thereby improving resistance to temperature induced viscosity reduction. Similarly, the relatively low slope observed for VFA-1 (–3.11) indicates that fly ash can also contribute to reducing viscosity susceptibility, possibly through its fine mineral particles and filler action within the binder system. Furthermore, the regression model had a very high coefficient of determination (R^2) (0.98–0.99), indicating that the regression equation was able to explain almost all the variation in viscosity data with temperature.

3.4. Viscoelastic performance analysis

In the unaged condition (Fig. 5 a), the complex shear modulus (G^*) values of all binders are quite high at low temperatures of 20–35 °C. However, as the temperature increases, the G^* value decreases to a very small value at temperatures above 60 °C. Micromaterial-modified binders show a slower decrease in G^* values in the temperature range of 20–40 °C, indicating that micromaterials help maintain initial stiffness by around 10–20%. In the RTFO condition (Fig. 5 b), all binders with micromaterial mixtures experience an increase in G^* values at low to medium temperatures of 20–40 °C, indicating good rutting resistance of around 5–20%. In contrast, VCr shows lower G^* values than pure binders, especially at low temperatures with a decrease of around

10–30%. The lower G^* of VCr does not necessarily indicate poorer performance, but rather reflects the development of a more compliant and elastic binder structure. In the PAV condition (Fig. 5 c), the G^* value increases at low to medium temperatures of 20–40 °C, indicating a long-term hardening effect due to oxidation of around 10–35%. Meanwhile, VCr exhibits a smaller stiffness gain in the PAV phase compared to mineral additives, approximately 5–15%. This result suggests that the elastomeric network formed by the swollen rubber particles may partially restrain the stiffening effect caused by oxidation and preserve the flexibility of the binder during long-term aging.

In the unaged state at intermediate temperatures, binders with VCe, VFA and VSi have a phase angle (δ) value lower by 2–5%, indicating stronger elastic properties and a more stable internal structure. Conversely, VCr has a significantly lower δ value, especially at high content levels, decreasing by 7–12%, indicating that rubber influences elasticity at low temperatures. As the temperature increases, all binders move towards higher δ values (approaching 90°). In the RTFO state, some modified binders have lower δ values than pure asphalt at low temperatures, with a decrease of 2–6%. In contrast, VCr exhibits a significantly lower δ value, 7–12%. In the PAV state, binders with VCe, VFA and VSi have lower δ values than pure asphalt, with decreases of 3–7%. VCr mixtures, especially VCr-3, showed the lowest δ values, namely 10–15%.

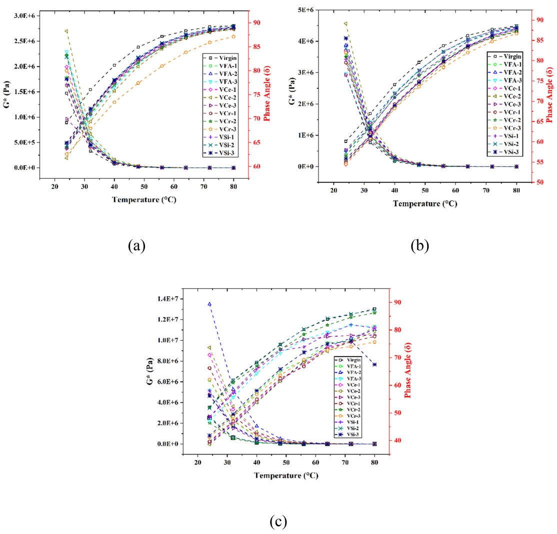

Fig. 5. Complex modulus (G^*) and phase angle (δ) for the binders (a) unaged; (b) RTFO-aged and (c) PAV-aged

3.5. Rheological performance analysis

The relationship between rutting ($G^* / \sin\delta$) and fatigue ($G^* \sin\delta$) to temperature and mixture percentage is shown in Fig. 6 and Fig. 7. In unaged and RTFO-aged conditions (Fig. 6 a and Fig. 6 b), it shows that all binders experience an 80–90% decrease in resistance to permanent deformation as the temperature increases from 40–80 °C. The addition of additive material in unaged conditions shows a decrease in $G^* / \sin\delta$ values in the medium temperature range of 40–60 °C. In RTFO conditions, it is seen that the decrease in $G^* / \sin\delta$ values is at medium temperatures of 50–70 °C.

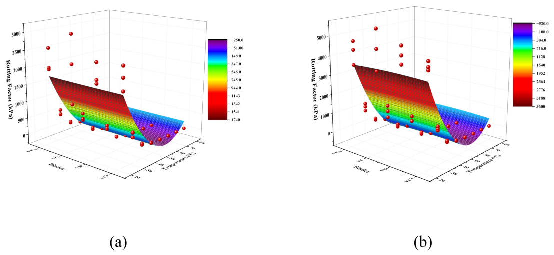

Fig. 6. Rutting performance ($G^* / \sin\delta$): (a) unaged and (b) RTFO-aged

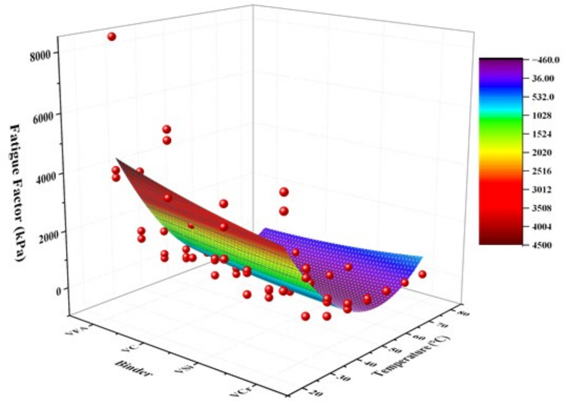

Fig. 7. Fatigue performance ($G^* \sin\delta$) at PAV-aged

The results for PAV-aged conditions (Fig. 7) show that all binders experienced a significant decrease in fatigue performance ($G^* \sin\delta$) as the temperature increased from 25–45 °C, with a decrease reaching 70–90%. This indicates a weakening of oxidative stiffness at intermediate temperatures after long-term aging. Compared to pure asphalt, almost all binders with additives showed lower fatigue factors, indicating increased resistance to fatigue cracking. VSi mixtures, especially VSi-1 and VSi-2, showed a decrease in $G^* \sin\delta$ values of 25–40% compared to pure asphalt. VFA and VCe showed a moderate decrease of 10–25%, in line with the character of inorganic fillers that are able to fill micro-voids and increase structural stability without completely reducing stiffness. VCr mixtures, especially VCr-3, had the lowest $G^* \sin\delta$ values, which were 45–60% lower than pure asphalt. These results indicate that the addition of elastomeric additives (Cr) is most effective in improving long-term fatigue resistance, while mineral additives (FA, Ce, and Si) provide optimal improvements by reducing oxidative stiffness and stabilizing the binder structure at medium temperatures.

3.6. Sensitivity analysis of rheological models

The sensitivity of the rutting and fatigue prediction models is shown in Table 5, which illustrates the relationships between predicted rutting and fatigue responses (y), temperature (T), and percentage (P) for various mixtures under three aging conditions. In general, all models follow a power law pattern, indicating that changes in temperature and percentage significantly influence the material response. In the unaged condition, all mixtures exhibit a very dominant temperature effect. This is evident from the large negative temperature exponents, ranging from −7.355 to −7.512. Negative exponents indicate that increasing temperature significantly decreases the material response. The percentage effect under these conditions shows significant variation between mixtures.

Table 5. Sensitivity of rheological prediction models

Materials	Unaged	R^2
VFA	$y = 5.64\text{e+}13 * T^{-7.409} * P^{0.157}$	0.986
VCe	$y = 5.46\text{e+}13 * T^{-7.355} * P^{0.07}$	0.978
VSi	$y = 7.995\text{e+}13 * T^{-7.512} * P^{0.015}$	0.988
VCr	$y = 4.51\text{e+}13 * T^{-7.381} * P^{0.306}$	0.988
	RTFO-aged	R^2
VFA	$y = 1.21\text{e+}13 * T^{-7.737} * P^{-0.119}$	0.982
VCe	$y = 1.33\text{e+}13 * T^{-7.363} * P^{-0.198}$	0.978
VSi	$y = 1.73\text{e+}13 * T^{-7.513} * P^{0.171}$	0.981
VCr	$y = 1.17\text{e+}14 * T^{-7.397} * P^{0.068}$	0.984
	PAV-aged	R^2
VFA	$y = 1.059\text{e+}13 * T^{-6.477} * P^{-0.174}$	0.921
VCe	$y = 9.03\text{e+}12 * T^{-6.341} * P^{-0.077}$	0.948
VSi	$y = 2.25\text{e+}13 * T^{-6.922} * P^{-0.073}$	0.917
VCr	$y = 8.65\text{e+}12 * T^{-6.549} * P^{-0.357}$	0.853

In the RTFO-aged condition, the temperature effect remains dominant. This is indicated by the relatively large temperature exponent values, ranging from −7.363 to −7.737. In the PAV-aged condition, the sensitivity to temperature decreases slightly compared to the previous condition. The temperature exponent values range from −6.341 to −6.922, indicating that the material becomes stiffer and reduces the effect of temperature on response changes. The effect of percentage shows a different pattern compared to the unaged condition. Some mixtures, such as VFA and VC, have negative percentage exponents, indicating that increasing the percentage decreases the material response value. The effect of percentage in this condition is negative for most mixtures, indicating that increasing the percentage tends to decrease the material response value. Based on the good R-square (R^2) value, the powerlaw model can still show good results for predicting rutting and fatigue values at each binder service life.

4. Conclusions

Based on the physical, rheological, and microstructural analysis results, the main findings of this study can be summarized as follows:

1. Each material has distinct microstructural characteristics that directly influence how the binder responds to modification. Si exhibits a reactive surface, Ce and FA are calcium-silica-rich, and Cr forms a porous elastomeric phase.

2. The addition of micro-material modifiers significantly influenced the physical characteristics of the asphalt binder through the reduction of penetration values and the increase of softening point temperatures. The VCr mixture exhibited the most significant reduction in penetration value, indicating an improvement in the balance between binder elasticity and stiffness, while VFA produced the highest increase in softening point, demonstrating better resistance to deformation at high temperatures.

3. Temperature and viscosity exhibited a strong relationship, indicating that the binder became more fluid at higher temperatures. Each binder showed different levels of temperature sensitivity, where some binders experienced faster changes in viscosity compared to others.

4. The viscoelastic evaluation results demonstrated that the addition of micromaterials improved the stiffness and elastic characteristics of the binders under various aging conditions. Modified binders with VCe, VFA, VCr and VSi exhibited an increase in complex modulus (G^*), particularly at low to intermediate temperatures. In addition, the reduction in phase angle (δ) indicated improved structural stability and elastic behavior of the binders. The VCr-3 mixture showed the lowest δ value with more dominant elastic enhancement, resulting in better fatigue resistance performance.

5. The rheological evaluation demonstrated that increasing temperature significantly reduced the rutting and fatigue performance under unaged, RTFO-aged and PAV-aged conditions. The rutting parameter ($G^* / \sin\delta$) showed a substantial reduction at high temperatures, while the fatigue parameter ($G^* \sin\delta$) decreased at intermediate temperatures after long-term aging, indicating increased thermal susceptibility and oxidative softening of the binder. Compared to the virgin binder, all modified binders exhibited lower $G^* \sin\delta$ values, indicating improved resistance to fatigue cracking. The VCr mixture, particularly VCr-3, demonstrated the most effective improvement in long-term fatigue resistance.

6. VCr provided superior temperature stability and elastic behavior, making it well-suited for pavements exposed to high service temperatures and heavy traffic loading, where rutting resistance is critical. VFA showed low temperature susceptibility and consistent rheological performance, suggesting potential as a cost-effective modifier for general applications. VCe and VSi mainly increased binder stiffness, making them suitable where higher structural rigidity is required; however, their greater temperature susceptibility should be considered in regions with significant temperature fluctuations.

Acknowledgements

The Faculty of Engineering Universitas Indonesia funded this research through the Regular Fundamental Research Program, financed by contract no. PKS-106/UN2.RST/HKP.05.00/2026. Directorate of Research and Community Service Directorate General of Research and Development Ministry of Higher Education, Science, and Technology. This research was conducted at the Structure and Material Laboratory of the Universitas Indonesia Civil Engineering Department.

References

[1] M. Lagos-Varas, A. C. Raposeiras, D. Movilla-Quesada, J. P. Arenas, D. Castro-Fresno, O. Muñoz-Cáceres, and V. C. Andres-Valeri, (2020) *"Study of the permanent deformation of binders and asphalt mixtures using rheological models of fractional viscoelasticity"* **Construction and Building Materials *260***: 120438. DOI: 10.1016/j.conbuildmat.2020.120438.

[2] A. B. Roy-Chowdhury, M. F. Saleh, and M. Moyers-Gonzalez, (2021) *"Characterisation of Permanent Deformation Behaviour of Asphalt Mix Based on a Combined Elastic Plastic (CEP) Parameter"* **Infrastructures *6***(12): 183. DOI: 10.3390/infrastructures6120183.

[3] S. P. Hadiwardoyo, R. J. Sumabrata, A. C. Nissa, F. A. Muhammad, M. Hia, D. Iskandar, and R. H. Lumingkewas, (2023) *"Improvement of Buton Rock Asphalt Performance by Adding Nano-Crumb Rubber and Waste Engine Oil"* **International Journal of Pavement Research and Technology *16***(5): 1181–1195. DOI: 10.1007/s42947-022-00189-4.

[4] X. Zhang, C. Han, J. Yang, X. Xu, and F. Zhang, (2021) *"Evaluating the Rheological Properties of High-Modulus Asphalt Binders Modified with Rubber Polymer Composite Modifier"* **Materials *14***(24): 7727. DOI: 10.3390/ma14247727.

[5] A. Behnood and M. Modiri Gharehveran, (2019) *"Morphology, rheology, and physical properties of polymer-modified asphalt binders"* **European Polymer Journal *112***: 766–791. DOI: 10.1016/j.eurpolymj.2018.10.049.

[6] R. Joumblat, Z. Al Basiouni Al Masri, and A. Elkordi, (2023) *"Dynamic Modulus and Phase Angle of Asphalt Concrete Mixtures Containing Municipal Solid Waste Incinerated Fly Ash as Mineral Filler Substitution"* **International Journal of Pavement Research and Technology *16***(5): 1196–1216. DOI: 10.1007/s42947-022-00190-x.

[7] I. S. Bessa, K. L. Vasconcelos, V. T. F. Castelo Branco, and L. L. B. Bernucci, (2019) *"Fatigue resistance of asphalt binders and the correlation with asphalt mixture behaviour"* **Road Materials and Pavement Design *20***(sup2): S695–S709. DOI: 10.1080/14680629.2019.1633741.

[8] M. A. Notani, P. Hajikarimi, F. M. Nejad, and A. Khodaii, (2020) *"Rutting resistance of toner-modified asphalt binder and mixture"* **International Journal of Pavement Research and Technology *13***(1): 1–9. DOI: 10.1007/s42947-019-0131-z.

[9] S. Sreedhar and E. Coleri, (2018) *"Effects of Binder Content, Density, Gradation, and Polymer Modification on Cracking and Rutting Resistance of Asphalt Mixtures Used in Oregon"* **Journal of Materials in Civil Engineering *30***(11): 04018298. DOI: 10.1061/(ASCE)MT.1943-5533.0002506.

[10] V. F. d. S. Neto, L. C. d. F. L. Lucena, A. G. de Barros, A. E. d. F. L. Lucena, and P. G. T. M. Filho, (2022) *"Rheological evaluation of asphalt binder modified with zinc oxide nanoparticles"* **Case Studies in Construction Materials *17***: e01224. DOI: 10.1016/j.cscm.2022.e01224.

[11] M. L. C. Aidara, M. Ba, and A. Carter, (2020) *"Impact of Intrinsic Properties of Aggregate and Volumetric Properties of Hot Mixture Asphalt (HMA) in the Influence of the Resistance to Rutting"* **Open Journal of Civil Engineering *10***(3): 187–194. DOI: 10.4236/OJCE.2020.103016.

[12] L. M. de Barros, L. A. H. do Nascimento, and F. T. S. Aragão, (2022) *"Effects of binder and aggregate properties on the permanent deformation of asphalt mixtures by means of uniaxial and triaxial tests"* **Construction and Building Materials *332***: 127346. DOI: 10.1016/J.CONBUILDMAT.2022.127346.

[13] Y. Yan, H. Zhang, M. Bekoe, C. Allen, J. Zhou, and R. Roque, (2023) *"Effects of asphalt binder type, aggregate type, and gradation characteristics on fracture properties and performance of asphalt mixtures at intermediate temperatures"* **Construction and Building Materials *409***: 133801. DOI: 10.1016/J.CONBUILDMAT.2023.133801.

[14] G. Tian, C. Chen, T. Zhang, Y. Gao, S. Wang, Y. Jia, Z. Chen, Y. Li, Z. Zhou, and Z. Wei, (2023) *"Effect of high-elasticity anti-rutting additive on viscoelastic behavior of asphalt binder and its modification mechanism"* **Case Studies in Construction Materials *19***: e02504. DOI: 10.1016/J.CSCM.2023.E02504.

[15] A. Behnood and M. Modiri Gharehveran, (2019) *"Morphology, rheology, and physical properties of polymer-modified asphalt binders"* **European Polymer Journal *112***: 766–791. DOI: 10.1016/J.EURPOLYMJ.2018.10.049.

[16] L. Porot, E. Chailleux, P. Apostolidis, J. Zhu, A. Margaritis, and L. Tsantilis, (2022) *"Complex Bituminous Binders, Are Current Test Methods Suitable for?"* **RILEM Bookseries *27***: 37–43. DOI: 10.1007/978-3-030-46455-4_5/SAVE-RESEARCH.

[17] Q. Liu, J. Wu, X. Qu, C. Wang, and M. Oeser, (2020) *"Investigation of bitumen rheological properties measured at different rheometer gap sizes"* **Construction and Building Materials *265***: 120287. DOI: 10.1016/J.CONBUILDMAT.2020.120287.

[18] F. S. Bhat and M. S. Mir, (2020) *"Rheological investigation of asphalt binder modified with nanosilica"* **International Journal of Pavement Research and Technology *14***(3): 276–287. DOI: 10.1007/S42947-020-0327-2.

[19] W. Haroon and N. Ahmad, (2024) *"Effect of nano silica on the performance of modified crumb rubber bitumen and asphalt mixtures"* **Innovative Infrastructure Solutions *9***(7): 280–. DOI: 10.1007/S41062-024-01590-7.

[20] G. Shafabakhsh, M. Motamedi, M. Firouznia, and M. Isazadeh, (2019) *"Experimental investigation of the effect of asphalt binder modified with nanosilica on the rutting, fatigue and performance grade"* **Petroleum Science and Technology *37***(13): 1495–1500. DOI: 10.1080/10916466.2018.1476534.

[21] H. H. Zghair, H. Jony, and M. Hassan. "Rheological Characteristics of Nano Silica Modified Asphalt Binder Material". In: *Proceedings of the 5th International Engineering Conference, IEC 2019*. Institute of Electrical and Electronics Engineers Inc., 2019, 79–84. DOI: 10.1109/IEC47844.2019.8950636.

[22] M. Saltan, S. Terzi, and S. Karahancer, (2018) *"Performance analysis of nano modified bitumen and hot mix asphalt"* **Construction and Building Materials *173***: 228–237. DOI: 10.1016/j.conbuildmat.2018.04.014.

[23] A. M. Al-Sabaeei, M. B. Napiah, M. H. Sutanto, W. S. Alaloul, S. E. Zoorob, and A. Usman, (2022) *"Influence of nanosilica particles on the high-temperature performance of waste denim fibre-modified bitumen"* **International Journal of Pavement Engineering *23***(2): 207–220. DOI: 10.1080/10298436.2020.1737060.

[24] B. Shi and S. Zhou, (2024) *"Application of fume silica nanoparticles to improve high-temperature rheological performance of terminal blend rubberized asphalt"* **Case Studies in Construction Materials *20***: e03276. DOI: 10.1016/j.cscm.2024.e03276.

[25] E. I. Szerb, I. Nicotera, B. Teltayev, R. Vaiana, and C. O. Rossi, (2018) *"Highly stable surfactant-crumb rubber-modified bitumen: NMR and rheological investigation"* **Road Materials and Pavement Design *19***(5): 1192–1202. DOI: 10.1080/14680629.2017.1289975.

[26] Rosnawati Buhari, S. S. Razi Zainal, N. H. Mohd Kamaruddin, and K. N. Yunos, (2024) *"Effect of Amine Additive on Rutting Resistance of Rubberized Asphalt Binder"* **Journal of Advanced Research in Applied Mechanics *123***(1): 135–146. DOI: 10.37934/aram.123.1.135146.

[27] R. M. Badri, Z. A. Alkaissi, and M. Sutanto, (2021) *"Physical, rheological and morphological characterization of modified asphalt binder with differing crumb rubber contents"* **Materials Today: Proceedings *42***: 3028–3034. DOI: 10.1016/J.MATPR.2020.12.819.

[28] S. J. Lee, C. K. Akisetty, and S. N. Amirkhanian, (2008) *"The effect of crumb rubber modifier (CRM) on the performance properties of rubberized binders in HMA pavements"* **Construction and Building Materials *22***(7): 1368–1376. DOI: 10.1016/j.conbuildmat.2007.04.010.

[29] M. Khalili, K. Jadidi, M. Karakouzian, and S. Amirkhanian, (2019) *"Rheological properties of modified crumb rubber asphalt binder and selecting the best modified binder using AHP method"* **Case Studies in Construction Materials *11***: e00276. DOI: 10.1016/J.CSCM.2019.E00276.

[30] N. K. Resentia, B. S. Subagio, E. S. Hariyadi, and R. G. Pradoto, (2023) *"Rheological Characteristic of Petroleum Asphalt Binder Modified by Natural Nano Silica and Nano Fly ash"* **International Journal of Pavement Research and Technology 2023 18:3 *18***(3): 577–585. DOI: 10.1007/S42947-023-00365-0.

[31] G. G. Al-Khateeb, A. Sukkari, H. Ezzat, E. Nasr, and W. Zeiada, (2024) *"Rheology of Crumb Rubber-Modified Warm Mix Asphalt (WMA)"* **Polymers *16***(7): 906. DOI: 10.3390/POLYM16070906.

[32] H. H. Zghair, H. H. Joni, and M. S. Hassan, (2019) *"Evaluation of the Effect of Mixing Conditions of Micro-Silica Modified Asphalt Binder"* **IOP Conference Series: Materials Science and Engineering *518***(2): 022048. DOI: 10.1088/1757-899X/518/2/022048.

[33] M. Saudy, M. Guirguis, S. ELBadawy, M. AbouZeid, and T. Madkour, (2026) *"A comparative evaluation of sustainable asphalt binder modifiers for enhanced performance"* **Scientific Reports *16***(1): 12213–. DOI: 10.1038/s41598-026-46495-w.

[34] A. A. Setiawan, F. J. Philip, E. Permanasari, and Resdiansyah, (2019) *"Skid Resistance and Micro-structure of Concrete Containing Waste Plastic Fiber for Rigid Pavement"* **Journal of Applied Science and Engineering *22***(4): 597–606. DOI: 10.6180/JASE.201912_22(4).0001.

[35] AASHTO T316. *Standard Method of Test for Viscosity Determination of Asphalt Binder Using Rotational Viscometer This document is only for acquaintance This document is only for acquaintance*. Tech. rep. 2019, 1–5. URL: https://matest.ru/uploads/standards/AASHTO_T316-13.pdf.

[36] AASHTO M320, (2015) *"Standard Specification for Performance-Graded Asphalt Binder This document is only for acquaintance This document is only for acquaintance"* **AASHTO Book of Standards *10***: 1–12. URL: https://matest.ru/uploads/standards/AASHTO_M320-15.pdf.

[37] R. L. Cosme, J. E. S. L. Teixeira, and J. L. Calmon, (2016) *"Use of frequency sweep and MSCR tests to characterize asphalt mastics containing ornamental stone residues and LD steel slag"* **Construction and Building Materials *122***: 556–566. DOI: 10.1016/J.CONBUILDMAT.2016.06.126.

[38] H. Nazari, K. Naderi, and F. Moghadas Nejad, (2018) *"Improving aging resistance and fatigue performance of asphalt binders using inorganic nanoparticles"* **Construction and Building Materials *170***: 591–602. DOI: 10.1016/J.CONBUILDMAT.2018.03.107.